A Postprocessing Methodology for Direct Normal Irradiance Forecasting Using Cloud Information and Aerosol Load Forecasts

J. L. CASADO-RUBIO, M. A. REVUELTA, M. POSTIGO, AND I. MARTÍNEZ-MARCO

Agencia Estatal de Meteorología, Madrid, Spain

C. YAGÜE

Department of Geophysics and Meteorology, Complutense University of Madrid, Madrid, Spain

(Manuscript received 1 September 2016, in final form 5 April 2017)

ABSTRACT

A method for direct normal irradiance (DNI) forecasting for specific sites is proposed. It is based on the combination of a numerical weather prediction (NWP) model, which provides cloud information, with radiative transfer simulations fed with external aerosol forecasts. The NWP model used is the ECMWF Integrated Forecast System, and the radiative transfer information has been obtained from the Library of Radiative Transfer (libRadtran). Two types of aerosol forecasts have been tested: the global Monitoring Atmospheric Composition and Climate (MACC) model, which predicts five major components of aerosols, and the Dust Regional Atmospheric Model (BSC-DREAM8b) added to a fixed background calculated as the 20th percentile of the monthly mean of AERONET 2.0 observations from a different year. The methodology employed is valid for all meteorological situations, providing a stable and continuous DNI curve. The performance of the combined method has been evaluated against DNI observations and compared with the pure ECMWF forecasts at eight locations in the southern half of mainland Spain and the Canary Islands, which received high loadings of African dust for 2013 and 2014. Results for 1-day forecasts are presented. Although clouds play a major role, aerosols have a significant effect, but at shorter time scales. The combination of ECMWF and MACC forecasts gives the best global results, improving the DNI forecasts in events with high aerosol content. The regional BSC-DREAM8b yields good results for some extremely high dust conditions, although more reliable predictions, valid for any aerosol conditions, are provided by the MACC model.

1. Introduction

Solar energy has become an increasingly important renewable source of electricity in the last decade worldwide, particularly in Spain (Kraas et al. 2013). It already provides approximately 5% of the electricity consumed in mainland Spain (REE 2015). Weather greatly affects the performance of solar power plants; therefore, transmission system operators (TSOs) need good meteorological forecasts to be able to predict the electricity supply curve in advance.

Solar energy can be converted into electricity using different technologies: directly from photovoltaics or indirectly through concentrating solar power (CSP). Photovoltaic plants depend mainly on global horizontal irradiance (GHI) for their operation, while CSP plants depend on direct normal irradiance (DNI). Different methods are used to predict these variables depending on the temporal scale considered. All-sky cameras, satellite images, neural networks, and cloud-tracking image analysis are useful for nowcasting and very short ranges, while numerical weather prediction (NWP) models are the best option for horizons beyond 6 h (Perez et al. 2010).

GHI is necessary for the models' energy budget, and thus model predictions of GHI have been available for many years. Perez et al. (2013) conducted a comprehensive comparison of the GHI predicted by several global, multiscale, and mesoscale models over the United States, Canada, and Europe. The European Centre for Medium-Range Weather Forecasts (ECMWF) model gave the best results, though an average of the models' output was even more accurate. DNI has not been traditionally an output parameter, but its vertical component, the direct horizontal irradiance (DHI), has recently begun to be predicted. This variable is very difficult to forecast, since direct irradiance

Corresponding author: Jose L. Casado-Rubio, jcasador@aemet.es

DOI: 10.1175/JAMC-D-16-0297.1

is greatly affected by clouds and aerosols. Besides, it is not trivial to predict the partitioning of global irradiance into the direct and diffuse parts. Lara-Fanego et al. (2012) assessed the hourly global and direct radiation predicted 1–3 days ahead by a mesoscale atmospheric model over southern Spain. They obtained a relative root-mean-square error for direct radiation up to 20% for clear days and 100% for cloudy days. Troccoli and Morcrette (2014) evaluated the 3-hourly DHI predicted 1–5 days ahead by the ECMWF model over Australia and estimated that a bias corrected DHI forecast might be used operationally during days with medium or low cloud cover.

A proper forecast of DNI requires not only improvements of cloud parameterization schemes but also the inclusion of aerosol sources by meteorological forecast models (Ruiz-Arias et al. 2014). Atmospheric aerosol content is not currently a prognostic variable in NWP models. Climatological values are used instead, thus NWP models cannot predict radiation changes due to aerosol variability. Nevertheless, the importance of including this information to improve the predictions of radiation variables has been recognized (Gleeson et al. 2016; Schroedter-Homscheidt et al. 2017), and the development of models with prognostic aerosols is an active field of research. The DNI, not the aerosol content, must be used to verify these improvements, in order to take into account the complex dependence of the DNI on solar zenith angle and aerosol type (Schroedter-Homscheidt et al. 2013).

The development of tools to include prognostic aerosols in the calculation of DNI forecasts is an active field of research. Breitkreuz et al. (2009) proposed combining NWP models for cloudy situations with radiation transfer calculations including aerosol forecasts for clear situations. These researchers classified the meteorological situation as clear or cloudy and used a different model in each case. Jimenez et al. (2016) developed an augmentation of the Weather Research and Forecasting (WRF) Model, WRF-Solar, which was specifically designed to meet the solar industry needs and provides direct and diffuse radiation forecasts, allows aerosol optical properties to change, and incorporates feedbacks between aerosols, solar irradiance, and clouds.

Following the approach used by Breitkreuz et al. (2009), we propose a similar methodology to obtain DNI forecasts, combining NWP and radiative transfer calculations in an integrated scheme, but without distinctions between clear and cloudy days. This method has been validated against six ground-based observation sites in the southern half of mainland Spain and two on the Canary Islands. This is a geographical area of great interest because of its solar resources and a mix of factors that impact the radiation: cloudiness, African dust outbreaks, and marine and anthropogenic aerosols, among others. The study is focused on one-day-ahead forecasts during daylight hours, an interval especially important for TSOs.

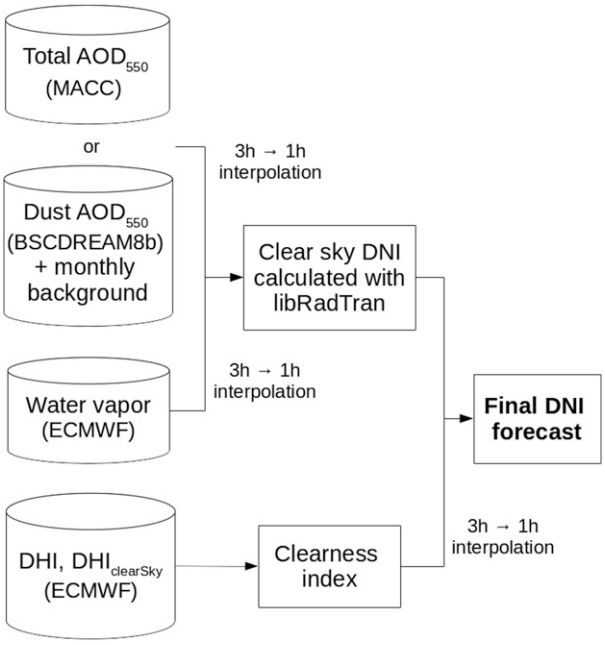

FIG. 1. Forecasting system scheme.

The paper is organized as follows: section 2 describes the methodology used, section 3 specifies the data used, section 4 details the results obtained, and the conclusions are shown in section 5.

2. Methodology

As discussed above, a method has been developed for the calculation of DNI forecasts for specific locations. The method relies on a NWP model to provide cloud information and on a radiative transfer model, fed with prognostic aerosols, to calculate clear-sky direct radiation.

In this work, the ECMWF Integrated Forecasting System has been chosen as NWP model. It incorporates a monthly climatology of aerosol loading, following Tegen et al. (1997). Thus, aerosol outbreaks are not taken into account. The Library of Radiative Transfer (libRadtran) is the radiative transfer model selected (Mayer and Kylling 2005), using the DISORT radiative transfer solver, described in Stamnes et al. (2000). Aerosol inputs are taken from the Monitoring Atmospheric Composition and Climate (MACC) model or Dust Regional Atmospheric Model (BSC-DREAM8b). However, the method can be used with different NWP and/or aerosol models, thus being very flexible. Figure 1 depicts the process flow of our system.

The proposed method calculates the DNI through the following equation:

$$\mathrm{DNI} = \mathrm{DNI}_{\mathrm{lRt}} \frac{\mathrm{DHI}}{\mathrm{DHI}_{\mathrm{clearSky}}}, \quad (1)$$

where

- $\mathrm{DNI}_{\mathrm{lRt}}$ is the instantaneous DNI calculated through libRadtran using as inputs the forecast water vapor content and the aerosol optical depth (AOD) and the default gases and ozone profiles from the standard input files provided by the model (sensitivity tests performed for each gas profile on selected days showed a small influence on DNI; surface pressure forecasts were also tested to take into account changes in the gas column, and the effect was found to be negligible),
- DHI is the NWP model direct horizontal irradiance, defined as the direct radiation passing through a flat horizontal plane and represented in the ECMWF model by the total sky direct solar radiation at surface, and
- $\mathrm{DHI}_{\mathrm{clearSky}}$ is the NWP model clear-sky direct horizontal irradiance, defined as the DHI under clear-sky conditions and represented in the ECMWF model by the clear-sky direct solar radiation at surface.

$\mathrm{DHI}/\mathrm{DHI}_{\mathrm{clearSky}}$ can be seen as a clearness index for the direct irradiance forecast by the ECMWF, similar to the clear-sky index defined by Girodo (2006) for global irradiation. This clearness index is defined as the ratio of two accumulated parameters over a time interval; hence it is not an instantaneous magnitude: it represents the cloudiness over the whole interval.

The above formula can be understood in two different ways: as the direct radiation predicted by libRadtran taking aerosols into account but modulated by the clearness index, which provides information about the NWP model cloudiness, or as the direct radiation predicted by the NWP model, but modulated by a second term that includes the effect of prognostic aerosols (the ratio of the libRadtran DNI and the clear-sky direct radiation).

The dependency of the atmospheric transmittance associated with the clouds with the solar zenith angle is considered indirectly, through the clearness index: the ECMWF model corrects the surface solar fluxes to take into account the change of the optical pathlength following Manners et al. (2009), as explained in ECMWF (2016).

To check the validity of our method several verification measures have been used, following the Management and Exploitation of Solar Resource Knowledge (MESOR) standard (Beyer et al. 2009): bias or mean error (ME), root-mean-square error (RMSE), and their relative counterparts rME and rRMSE (score divided by the mean of the observed DNI) have been calculated. DNI is highly variable, both in space and time, and prone to errors in location. To minimize the RMSE, we have considered the forecast averaged over different areas around the site, to smooth the effect of clouds. The area depends on the orography, among other factors, and is also highly variable for the sites studied in this work, as will be detailed in the results section.

To conduct this study, DNI has been calculated with libRadtran every hour for the first 24 h and has been corrected with the clearness index calculated from ECMWF model data. Sunrises and sunsets have been excluded: only zenith angles in the range of 0°–82° have been considered to avoid possible shadows. Furthermore, the direct solar radiation outside that interval is below 200 $\mathrm{W\,m^{-2}}$ and no substantial electricity is produced by CSP plants during those periods (Schroedter-Homscheidt et al. 2013).

3. Data

a. *Model data*

1) ECMWF MODEL

Operational forecasts of the total and clear-sky direct solar radiation at the surface from the high-resolution ECMWF model 0000 UTC runs, taken every three hours, have been used to calculate the clearness index (ratio of these two quantities) used in our algorithm. The 3-h interval has been chosen since it is the frequency available to commercial users. The clearness index has been subsequently interpolated linearly to get forecasts every hour. In addition, the total column water vapor from ECMWF has been used as an input parameter for the libRadtran model.

On the other hand, the hourly ECMWF total direct solar radiation at the surface has been used as a reference with which to compare the performance of our method. This variable is accumulated, so it has been divided by the corresponding period of time (1 h) to get instantaneous values. To be able to compare it with DNI observations it has been converted into DNI dividing it by the cosine of the solar zenith angle (SZA):

$$\mathrm{DNI} = \frac{\mathrm{DHI}}{\cos(\mathrm{SZA})}. \quad (2)$$

The SZA varies substantially over 1 h, and the best practice for choosing this angle is not straightforward (Blanc and Wald 2016). In this work we have chosen the simplest method, taking the value of instantaneous SZA halfway through the interval as the representative value.

The nearest point to each location has been selected using a 0.125° grid, the maximum ECMWF model

spatial resolution. The lead times considered are in the range of 0–24 h.

2) AEROSOL MODELS

Forecasts of AOD at 550 nm (AOD550) have been retrieved from two different sources: the global MACC model and the regional BSC-DREAM8b.

The MACC program (http://www.gmes-atmosphere.eu) intends to establish an atmospheric environmental service within the European Copernicus program to record, monitor, and forecast the air quality and atmospheric composition, among other conditions. Near-real-time AOD forecasts from MACC include 5 main aerosol types: sea salt, sulfate, dust, organic matter, and black carbon. The natural aerosols (sea salt, dust and dimethyl sulfide, the main natural precursor of sulfate) have their sources linked to some prognostic and diagnostic model variables. On the other hand, the anthropogenic aerosols (organic matter, black carbon and sulfate) are climatological values read from external datasets (Morcrette et al. 2009, 2011). The 0.25° spatial resolution data from the 0000 UTC runs for 0–24-h lead times have been used as inputs of libRadtran.

BSC-DREAM8b is a model focused on dust (Basart et al. 2012), part of the ensemble used by the WMO Sand and Dust Storm Warning Advisory and Assessment System (SDS-WAS) framework to provide dust forecasts for the northern Africa–Middle East–Europe area (http://sds-was.aemet.es). While in MACC the potential dust emission is independent from the soil morphology, in BSC-DREAM8b soil textures are considered. The spatial resolution is 0.33°. The 1200 UTC runs for 12–36-h lead times have been used as input for libRadtran. An AOD background has been added to the BSC-DREAM8b forecast to account for the aerosol constituents not predicted by the model. This background has been calculated as the 20th percentile of the monthly mean of AERONET 2.0 observations from nearby stations. Most AERONET datasets were only available since 2013, hence the 2014 background has been estimated from 2013 observations, and the 2013 background has been estimated from 2014 observations.

For both models the forecasts were available at 3-h intervals, so they have been interpolated linearly in time to get hourly data to feed libRadtran.

b. *Observational data*

DNI ground measurements from the Spanish Meteorological Service [Agencia Estatal de Meteorología (AEMET)] radiation network have been used to quantify the accuracy of the forecasts. Eight stations from this network have been selected: Albacete (39.00°N, 1.87°W), El Arenosillo (37.10°N, 6.74°W), Badajoz (38.88°N, 7.01°W), Cáceres (39.47°N, 6.34°W), Madrid (40.45°N, 3.72°W), and Murcia (38.0°N, 1.17°W) in southern mainland Spain and Maspalomas (27.76°N, 15.58°W) and Santa Cruz de Tenerife (28.46°N, 16.26°W) in the Canary Islands. These stations have Kipp and Zonen pyrheliometers, calibrated according to global standards, for the direct measurement of DNI. Irradiance data have been acquired every minute and afterward have been aggregated into 1-hourly totals. The period covered spans from 1 January 2013 to 31 December 2014, during daylight hours.

In addition, AOD at 500 nm measured at five stations belonging to the AERONET network at the 2.0 level [Badajoz, Madrid, Murcia, Huelva (situated at 37.02°N, 6.57°W, close to El Arenosillo), and La Laguna (situated at 28.48°N, 16.32°W, close to Tenerife)] have been used to calculate monthly aerosol backgrounds to add to the BSC-DREAM8b dust forecast. They have been also used to enable separate analysis of both clear and cloudy situations.

4. Results and discussion

a. *Clearness index spatial resolution*

The optimal spatial resolution of the clearness index depends on the geographical and meteorological conditions of every location. We have studied the variation of the RMSE of the DNI prediction calculated with (1) against the grid size to select the best grid area. Figure 2 shows the dependence of the RMSE and RMSE/RMSE0 with increasing grid area for 2013 and 2014 for the eight sites studied. RMSE0 represents the root-mean-square error taking only the grid point closest to the site. Hourly time series for both years have been used for this analysis. The grid area was varied from 0 km (the grid point closest to the site) to 350 km (784 points). Note that for the RMSE/RMSE0 curve the vertical axis is only represented between 0.94 and 1 to better indicate the slope.

Results from 2013 demonstrate that the RMSE exhibited a greater dispersion, with values between 175 and 300 $W\,m^{-2}$, whereas in 2014 the continental sites were grouped in a band of 180–210 $W\,m^{-2}$ while the island sites showed values around 275 $W\,m^{-2}$. The error was significantly higher for island sites because only large-scale cloud features, associated with the trade winds regime, were well predicted. Mesoscale cloud patterns are not captured because of the relatively small land area of the Canary Islands, and their rough and steep orography, not represented accurately by the current ECMWF model. This problem was especially evident in Santa Cruz de Tenerife, which is close to the border between the northern cloudy part of Tenerife and the southern sunnier part.

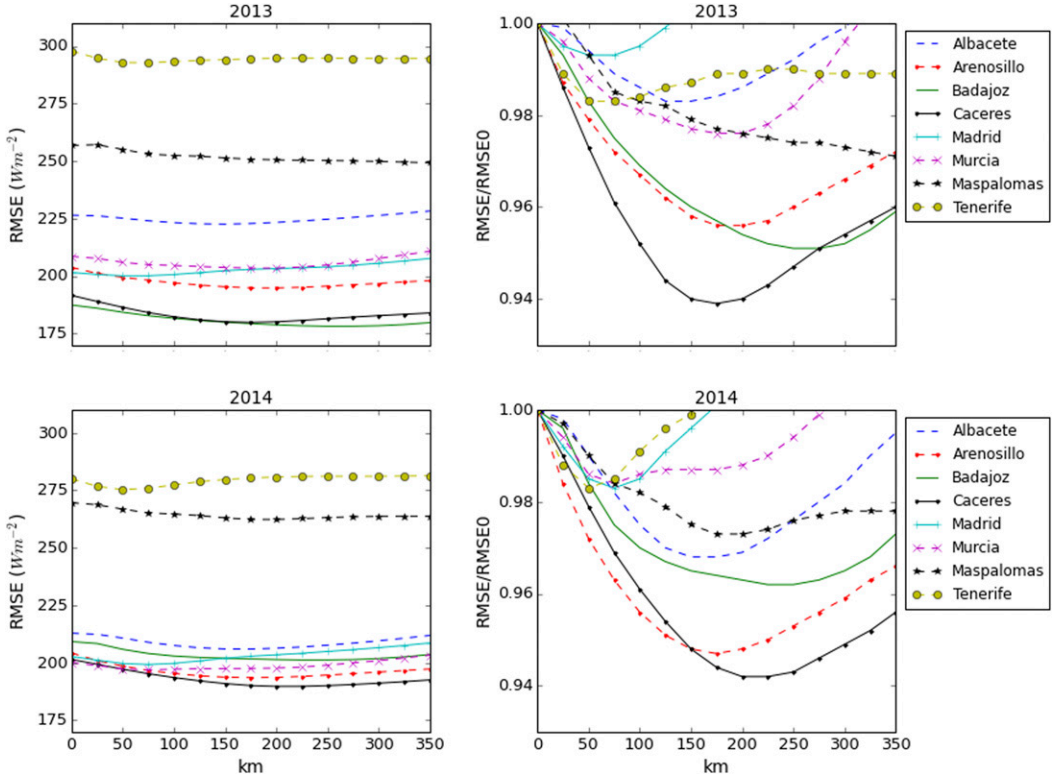

FIG. 2. (left) RMSE vs grid size and (right) RMSE/RMSE0 vs grid size for the combined method validated against observations.

The RMSE scaled by the RMSE0 shows the dependence on grid area more clearly. In general, the error decreased as the area increased up to some limit where they started to rise, although some of them showed a wavy behavior (Murcia). The grid area for which the minimum RMSE was reached was highly dependent on the site. Madrid and Tenerife presented the minimum value at the smallest area (50–75 km). In contrast, Badajoz reached the minimum at the largest size area (225–250 km).

The relationship between the orography, the grid area used to compute the clearness index and the minimum RMSE was investigated. The distance from every site to the closest mountain chain was estimated to be in a range of 10–200 km. The four inland sites (Albacete, Badajoz, Cáceres, and Madrid) showed a clear positive correlation between the grid area size and the distance to the closest mountains. This correlation was smaller when we considered coastal sites.

For the rest of the work, a square with a side length of 50 km (comprising 25 grid points) has been chosen to average the clearness index, unless otherwise specified. Although several sites would get a lower RMSE if a larger square was used, this is not guaranteed to happen for every location: 50 km is the smallest value that optimizes the performance of our method for all the sites in the sampling period studied. Furthermore, the computational effort necessary to perform the calculations is affordable for an operational product if a 50-km-side square is used.

b. *Annual scores*

Scores have been evaluated annually to do an initial comparison of the DNI forecast by the ECMWF model on one side, and the DNI calculated by our combined method on the other.

Many studies put the focus on the radiative effects and importance of mineral dust (Tanré et al. 2003; Nabat et al. 2015). To study this aspect in detail, our combined method was tested using three different AOD sources to feed libRadtran: the total AOD from MACC (cMACCt), which includes the five aerosol types, the AOD due to dust from MACC (without the other components) plus a monthly background (cMACCd), and the AOD due to dust from BSC-DREAM8b plus a monthly background (cDREAM8b). The comparison between the results obtained with cMACCt and cMACCd (or cDREAM8b) allows us to evaluate the role played by the other four aerosol major components modeled (sea salt, black carbon, organic matter, and sulfate).

Table 1 shows the rME and rRMSE using all these methods as well as the rRMSE for the 1-day persistence.

TABLE 1. Annual rME and rRMSE for eight locations (%).

Site	Year	ECMWF	cMACCt	cMACCd	cDREAM8b	(rME) or (rRMSE)	Persistence
				rME			
Albacete	2013	17.8	18.1	21.0	22.1	−1.9	—
Badajoz	2013	12.2	10.5	17.1	18.5	14.2	—
Caceres	2013	7.8	7.2	12.9	14.1	7.9	—
El Arenosillo	2013	16.5	10.9	17.2	18.5	33.8	—
Madrid	2013	9.2	7.6	12.9	13.7	17.4	—
Murcia	2013	12.5	12.5	16.0	17.0	0.0	—
Maspalomas	2013	32.3	20.1	24.5	29.0	37.9	—
Tenerife	2013	18.6	10.7	15.0	18.8	42.5	—
Albacete	2014	21.4	21.1	25.3	26.5	1.6	—
Badajoz	2014	17.2	14.7	20.9	21.3	14.7	—
Caceres	2014	12.6	11.5	17.1	17.5	9.0	—
El Arenosillo	2014	17.6	12.5	17.7	18.7	28.5	—
Madrid	2014	11.4	9.2	13.3	13.9	18.8	—
Murcia	2014	14.5	12.7	17.7	19.5	12.2	—
Maspalomas	2014	33.7	25.9	31.5	32.8	23.2	—
Tenerife	2014	9.8	5.0	9.9	12.8	49.3	—
Avg		16.6	13.1	18.1	19.7	19.3	—
				rRMSE			
Albacete	2013	50.1	47.3	49.3	49.9	5.6	74.7
Badajoz	2013	40.7	35.5	39.2	40.0	12.7	63.3
Caceres	2013	39.5	34.5	37.2	37.6	12.7	63.3
El Arenosillo	2013	42.4	36.9	40.8	41.5	12.8	64.5
Madrid	2013	43.2	38.7	41.3	41.7	10.4	69.6
Murcia	2013	42.5	39.2	41.9	42.7	7.8	68.8
Maspalomas	2013	56.4	50.2	53.0	55.1	11.0	60.7
Tenerife	2013	65.8	62.2	63.8	64.7	5.4	71.6
Albacete	2014	47.6	43.6	46.6	47.5	8.4	69.8
Badajoz	2014	47.7	42.3	46.2	46.5	11.4	70.9
Caceres	2014	43.2	39.3	42.2	42.5	9.0	68.9
El Arenosillo	2014	42.7	37.1	40.5	41.0	13.1	63.4
Madrid	2014	43.1	39.5	41.2	41.7	8.3	70.4
Murcia	2014	41.7	37.4	39.8	41.1	10.5	65.8
Maspalomas	2014	60.8	55.8	58.4	59.4	8.3	64.5
Tenerife	2014	58.6	55.1	56.7	57.4	5.9	72.2
Avg		47.9	43.4	46.1	46.9	9.6	67.7

The terms Δ(rME) and Δ(rRMSE) represent the difference between the score for the pure ECMWF forecast and the score corresponding to our method with the total MACC AOD (cMACCt), divided by the former:

$$\Delta(\mathrm{rME}) = \frac{\mathrm{rME}_{\mathrm{ECMWF}} - \mathrm{rME}_{\mathrm{cMACCt}}}{\mathrm{rME}_{\mathrm{ECMWF}}} \quad \text{and}$$

$$\Delta(\mathrm{rRMSE}) = \frac{\mathrm{rRMSE}_{\mathrm{ECMWF}} - \mathrm{rRMSE}_{\mathrm{cMACCt}}}{\mathrm{rRMSE}_{\mathrm{ECMWF}}}. \quad (3)$$

Positive values of Δ(rRMSE) indicate our combined method gave better results than the ECMWF model. The annual improvement in rRMSE was in the range 5%–13% using the total AOD from MACC. Best results were achieved by both the ECMWF model and our method in mainland Spain (35%–45% of rRMSE if the total AOD from MACC is used). The scores shown here are consistent with the results presented by Wittmann et al. (2008) using the method described in Breitkreuz et al. (2009), and also with the verification of ECMWF in Schroedter-Homscheidt et al. (2017). Using the 1-day persistence gave worse results for all the sites.

Positive bias showed that in all stations studied both models overestimated the annual mean direct irradiance. The scores for the stations of Maspalomas and Tenerife were poorer because of the difficulties of cloud forecasting on these islands. Nonetheless, the Canary Islands are exposed to very high levels of African dust. Several times every year, dust episodes can last more than 15 days. The SDS-WAS identified 193 days with African dust intrusions affecting the particulate matter levels on surface during 2013 and 2014, which means 26% of days. Hence the combined method was expected to provide significant

benefits. These benefits were found in Maspalomas, being the site in which the combined method showed the highest improvements, but not in Tenerife. This can be explained by the geographical location of each station: Maspalomas is in the southern part of the island, where the annual solar insolation is very high and there are few cloudy days, whereas Tenerife is close to the mountains in an area in which cloud forecasting is especially difficult because of the interaction of the trade winds with the mesoscale terrain. Furthermore, Maspalomas is closer to the African continent, so it is more affected by dust events.

In mainland Spain, the highest improvements were registered in El Arenosillo, which is also located in an area that receives high African dust loadings. The SDS-WAS identified 147 days with African dust intrusions during 2013 and 2014, which represents 20% of days. Similar frequencies of dust episodes were received in Murcia (132 days—18%). In contrast, only 90 days with African events (12%) reaching the center of the Iberian Peninsula were identified.

The rRMSE using just the dust AOD from MACC or BSC-DREAM8b (plus an aerosol background) was rather similar for both sources and only slightly lower than the ECMWF rRMSE. This was caused by the higher bias of both sources when compared with the ECMWF bias. Although these sources take into account the variability of the dust content and consequently improve the DNI forecasts, their performance was reduced by a less well-tuned aerosol background.

Figure 3 depicts the spatial distribution of the Δ(rRMSE) as a percentage for 2013 and 2014. In mainland Spain, the difference between the use of dust only and the five aerosol types was considerable. In the Canary Islands this difference was much smaller, although a more complete aerosol description was also beneficial. For cMACCt, in both years the improvement was higher in the western part of the Iberian Peninsula. In 2013 the improvement was smallest in the east, while in 2014 the poorest performance was registered in the northern stations. For cMACCd the smaller improvements appeared to be more randomly distributed.

c. *Monthly evolution*

To verify the performance of the method for different seasons, we have studied the monthly evolution of the scores jointly with the input parameters.

Figure 4 depicts the monthly improvement in rRMSE achieved with the combined method with respect to the results obtained by the ECMWF alone for 2013 and 2014 in five of the eight stations (El Arenosillo, Badajoz, Madrid, Murcia, and Maspalomas). The monthly averaged AOD at 500 nm (AOD500) observed by AERONET is also shown (green upside-down triangles) when available. These data have been obtained from the CAELIS tool (http://www.caelis.uva.es/). In Maspalomas, AERONET data from La Laguna station have been used. Note that the monthly AOD mean may not be representative for certain months (e.g., the sample was very small in La Laguna for September 2014), and there are no data for El Arenosillo.

The effect was positive for the whole two years when the total AOD from MACC was used. The Δ(rRMSE) reached up to 25% in Maspalomas, which can be attributed to the very large dust loading. The monthly evolution using both aerosol models followed a similar curve, which highlights the relevance of the dust contribution. However, BSC-DREAM8b (orange circles) did not always improve the prediction and even gave worse results, probably because the background value taken was too low. This means that dust models can be useful for radiation forecasting in some areas when dust accounts for a high proportion of the total aerosols, but in general more complete aerosol descriptions are needed.

In mainland Spain, the highest values for Δ(rRMSE) (close to 20%) were obtained in winter and seem to be associated more with the smoothing of cloudiness implied by our method than with the AOD correction. The improvement in rRMSE was not correlated with the observed AOD. Only in Maspalomas was the monthly evolution of both parameters similar. In contrast, high correlations were found between the rRMSE and the total cloud cover forecast by the ECMWF. Correlations larger than 0.74 were found for all the peninsular stations and years and larger than 0.90 for the four inland locations: Badajoz, Cáceres, Madrid, and Albacete in part of the period studied. These correlations were significantly lower on the islands.

To ascertain the relative importance of the smoothing throughout the year, the monthly Δ(rRMSE) using the MACC model total AOD was plotted for different clearness index averaging areas (Fig. 5). For El Arenosillo and Badajoz, there were marked improvements in autumn and winter when bigger smoothing areas were used, especially during months with large errors. On the other hand the impact of the averaging was negligible in Murcia, and less pronounced in Madrid and Maspalomas, indicating a prevalence of a spatially uniform cloud cover in some cases or a higher aerosol content in others.

In conclusion, the DNI output depended very strongly on the cloud forecasts, though this influence varied from one region to another. The influence of the aerosols was clear only in locations with a very high proportion of sunny days, such as Maspalomas. It is necessary to study clear-sky situations separately to assess the effect of the combined method.

d. *Cloudless situations*

Table 2 shows the scores for clear-sky hours. Situations have been selected that fulfilled two conditions: an

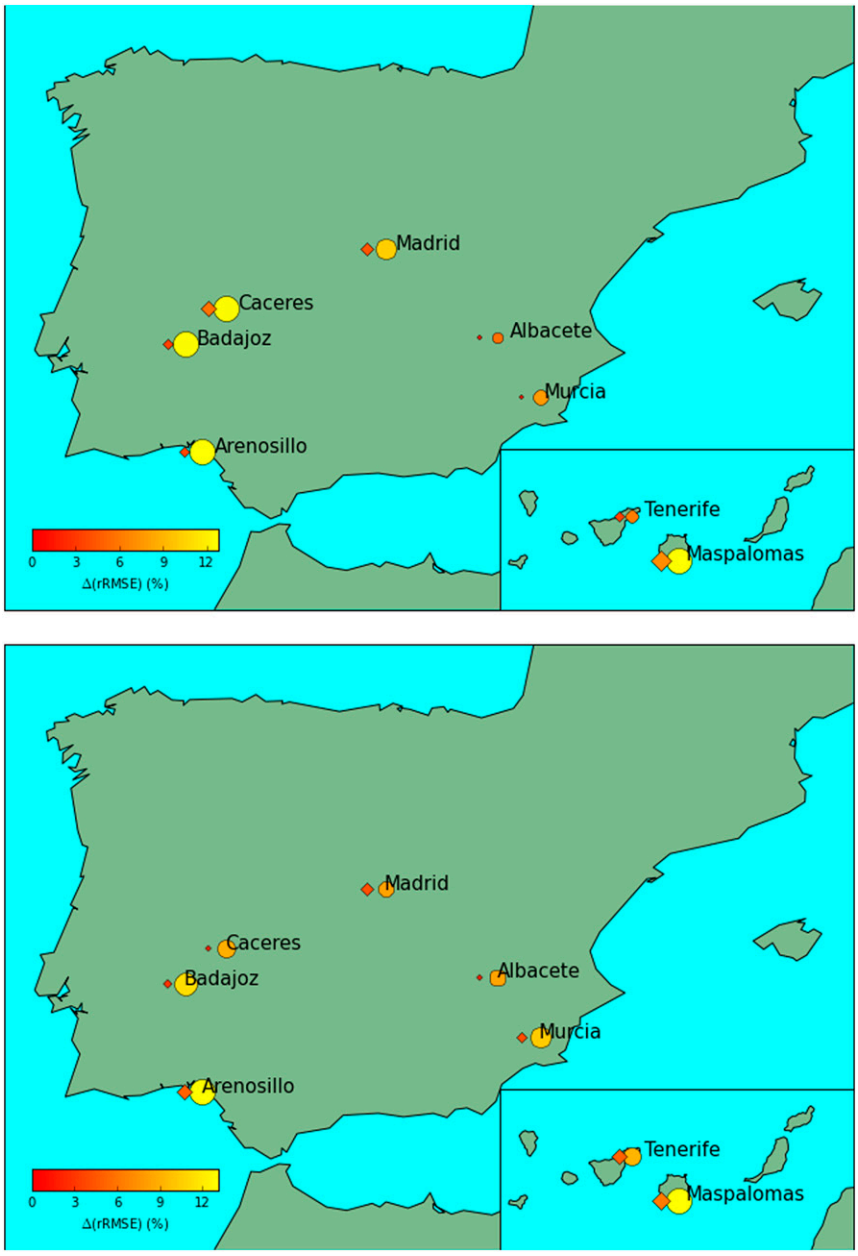

FIG. 3. The Δ(rRMSE) between the ECMWF and the combined method with MACC for (top) 2013 and (bottom) 2014 in the eight locations. Larger bright markers indicate larger values; cMACCt is given by circles, and cMACCd is given by diamonds.

observational one—the availability of AERONET 2.0 data—and a forecasting one—that the total cloud cover forecast by the NWP model was below 10%. These conditions have been imposed to avoid errors due to inaccurate cloud forecasts and put the focus on the performance of our method for clear-sky conditions. Also, they have been used in the past (Breitkreuz et al. 2009; Schroedter-Homscheidt et al. 2013). AERONET 2.0 AOD data were available only in three of the stations studied in this paper (Badajoz, Madrid, and Murcia), so the verification of the method for cloud-free situations has been restricted to them.

The rRMSE values in this case were dramatically lower than the ones found for all meteorological situations, reflecting again the major role of cloudiness in radiation studies (Lara-Fanego et al. 2012). They were very similar (5%–15% of error) to the values found by Schroedter-Homscheidt et al. (2013), who also fed

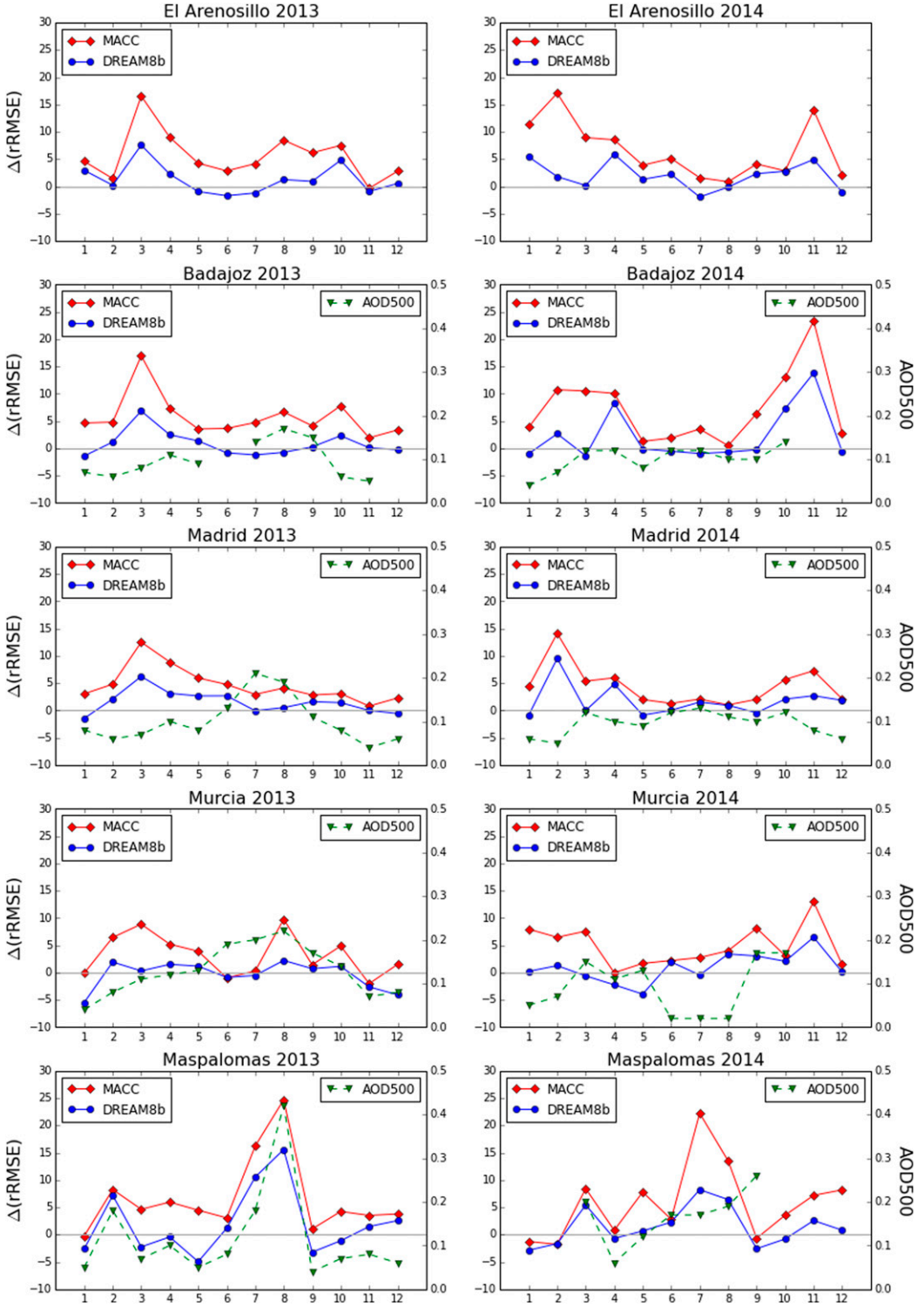

FIG. 4. Difference in rRMSE (%) using libRadtran with MACC (red diamonds) or with BSC-DREAM8b + background (blue circles) with respect to the pure ECMWF model. Also shown is AOD500 from AERONET (green upside-down triangles).

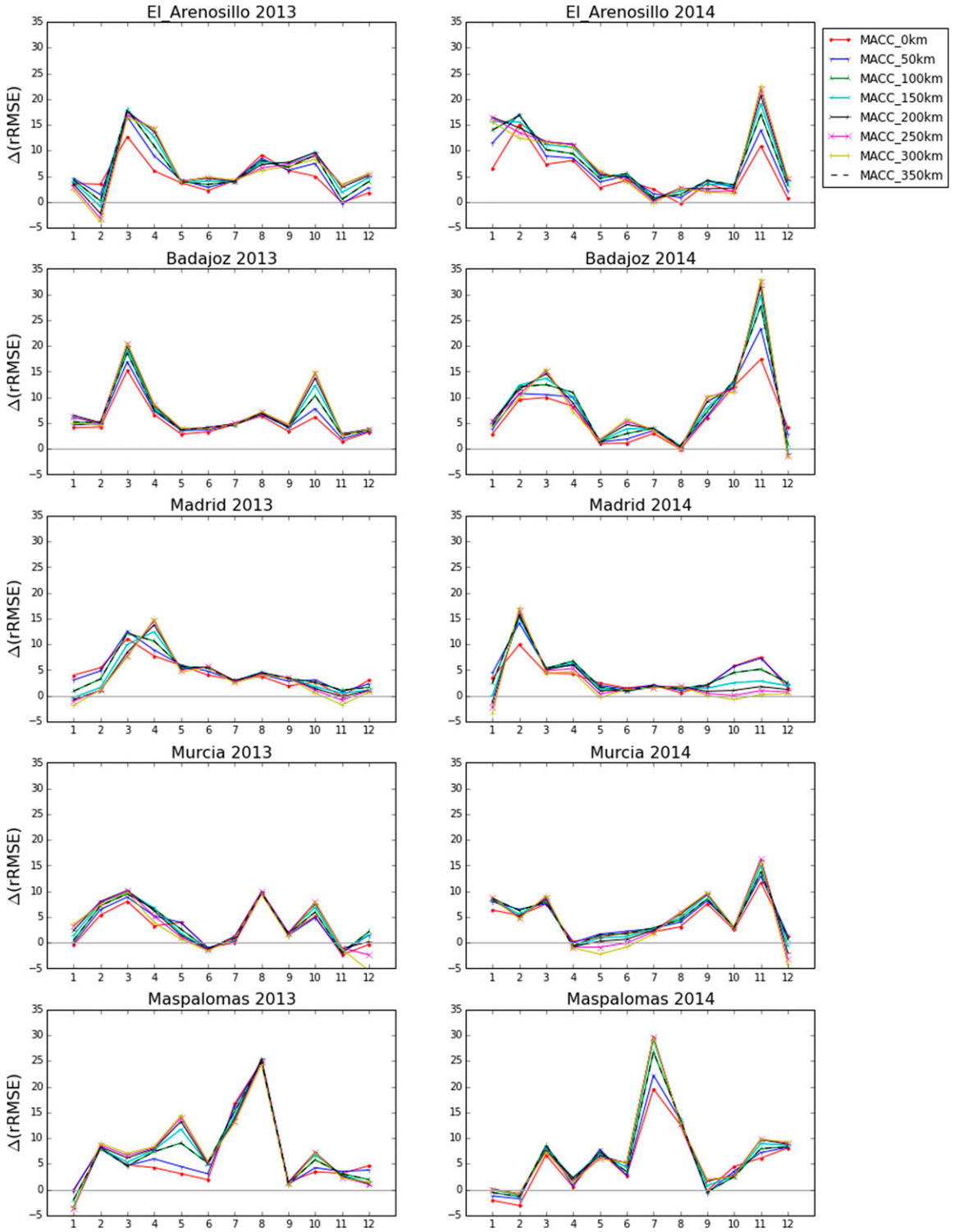

FIG. 5. Difference in rRMSE (%) using libRadtran with MACC (red diamonds) for eight different clearness index averaging areas ranging from 0 to 350 km.

TABLE 2. Relative RMSE and DNI reduction for clear-sky situations (%).

Site	Year	No. clear hours	rRMSE (ECMWF)	rRMSE (cMACCt)	rRMSE (cDREAM8b)	% DNI reduction
Badajoz	2013	881	9.8	8.1	10.5	7.0
Madrid	2013	928	12.9	11.2	11.3	5.6
Murcia	2013	1200	10.6	9.6	9.7	10.9
Badajoz	2014	987	8.6	6.8	7.3	5.9
Madrid	2014	920	9.3	9.1	8.6	5.6
Murcia	2014	1096	11.0	9.4	9.0	11.9
Avg		1002	10.4	9.0	9.4	7.8

libRadtran with MACC data to get DNI forecasts for clear-sky days.

Improvements have been found for both MACC and BSC-DREAM8b models in 2014. In 2013, maybe because of a lesser impact of African dust outbreaks in western Spain, the use of BSC-DREAM8b + background did not improve the ECMWF results in Badajoz. Table 3 shows the percentage of dust in total aerosol estimated from AERONET data for five stations.

The column % DNI reduction in Table 2 has been calculated as the difference between the DNI simulated in absence of aerosols—incorporating just the forecast water vapor content and standard gases profiles—and the DNI observed.

It gives a rough indication of the importance of aerosols for the DNI. For the cloudless situations selected it represented 5%–12% of the yearly decrease. Murcia is the station where this percentage was higher because of the larger impact of African dust outbreaks in the southeast of mainland Spain. Note that the selection did not include all the cloudless situations.

e. *High aerosol load events*

A situation has been classified as a high aerosol load event when its AOD was higher than the 85th percentile of the AOD500 measured by AERONET. In these situations the improvements achieved by the combined method are expected to be the highest. Results of the scores found for these cases are presented in Table 4. The scores were poorer than the ones obtained for the clear-sky situations because of the difficulties in aerosol forecasting. The best predictions were achieved using the MACC total AOD. However, the results found using the BSC-DREAM8b dust regional model were very similar for some events, reflecting the importance of dust outbreaks.

The results achieved with the MACC total AOD were considerably better in 2013 than in 2014. On average Δ(rRMSE) was 30% for the first year and 24% for the second. However, this behavior cannot be attributed to higher AOD levels or a larger proportion of dust, since the number of hours with high AOD was similar in both years. It has to do with the temporal distribution of large aerosol concentrations. During 2013 the high aerosol events were more concentrated in the summer months, with long continuous periods with high AOD values. In contrast, in 2014 they were distributed more evenly over the year and lasted a shorter time. These situations are much more challenging for models. To obtain a quantitative estimation of this behavior the temporal standard deviation σ of situations with high aerosol content was computed. This statistic has been defined as the standard deviation of the distribution obtained by selecting the hours of the year (using the day as time unit) where the AOD reaches or surpasses the 85th percentile. The maximum possible value for σ is approximately 105.4 days, which happens if the high aerosol events are distributed evenly through the year. It was observed that σ was far lower in 2013 than in 2014 in Madrid and Badajoz, indicating that the high aerosol events were more concentrated in time during that year. In contrast, the difference between 2013 and 2014 was small in Murcia, and accordingly Δ(rRMSE) was similar for both years.

f. *Hourly evolution: Case studies*

In this section two case studies corresponding to two interesting meteorological situations are presented.

The first case represents an example of the behavior of the combined method during an 8-day period with clear and cloudy days and high aerosol loadings in Murcia (Fig. 6). From 14 to 17 June 2013 the SDS-WAS identified an African dust intrusion reaching the southeastern part of mainland Spain. A gradual reduction in DNI occurred, which can be associated with the radiation dispersion by dust in the atmosphere. The DNI

TABLE 3. Percent of dust in total aerosol (source: http://www.caelis.uva.es/).

Site	2013	2014
Badajoz	3.6	5.7
Madrid	4.4	7.0
Huelva (El Arenosillo)	10.3	—
Murcia	14.1	21.5
La Laguna (Tenerife)	20.4	36.7

TABLE 4. Relative RMSE in high aerosol content events (%), number of hours, and standard deviation of high AOD events.

Site	Year	No. high AOD hours	σ(days)	rRMSE (ECMWF)	rRMSE (cMACCt)	rRMSE (cDREAM8b)	Δ(rRMSE)
Badajoz	2013	182	35.7	21.2	13.7	22.3	35.4
Madrid	2013	206	22.6	18.9	13.3	16.3	29.5
Murcia	2013	270	46.6	24.0	17.5	21.1	27.1
Badajoz	2014	201	60.7	19.5	14.5	16.9	25.9
Madrid	2014	224	70.4	19.0	15.0	15.6	21.0
Murcia	2014	245	56.3	23.6	17.4	19.4	26.2
Avg		221	48.7	21.0	15.2	18.6	27.5

reduction reached its maximum value on 16 June, with up to 16% at noon. It can be observed that from 15 to 17 June 2013 the ECMWF model overestimated direct irradiance, since the model was not able to account for aerosol load variations. In contrast, the combined method followed the observed DNI closely.

On 17 June cloudiness developed in the area and the clearness index dropped, sometimes reaching values close to zero. In contrast with the smooth decrease registered during the course of the dust event, the DNI hourly evolution curve showed abrupt changes. In this type of meteorological situations the DNI forecast is particularly challenging. The combined method modulated the ECMWF response taking into account the aerosol load and showed a smoother variation since it is based on forecasts at 3-h intervals. Although the combined method could not follow the DNI variations as closely as in the cloudless days, it succeeded again in providing a realistic forecast.

This example highlights one of the strengths of the combined method we have used: although other methods have been developed to improve clear-sky DNI forecasts (Breitkreuz et al. 2009; Martin-Pomares et al. 2015), they rely on an artificial dual classification of the meteorological situations as ''clear'' or ''cloudy,'' which makes it very difficult to obtain a stable and continuous DNI forecast like the one shown in Fig. 6.

The second case is an example of a very intense African outbreak in the Canary Islands for clear-sky conditions, which took place from 8 to 18 July 2013. Figure 7 depicts the first two days, when the strongest drop in DNI occurred in Maspalomas. The DNI reduction was as high as 46% at noon. The ECMWF forecast showed a poor performance because of the lack of aerosol forecasting, but, when combined with an aerosol model, it improved substantially (over 80% decrease in rRMSE using BSC-DREAM8b in this particular case). Schroedter-Homscheidt et al. (2013) found that these types of severe events are rare (deviations of 20% DNI only happen around 10% of hours) and have a small influence on scores but can affect electricity generation significantly, especially in dust-dominated sites like Maspalomas. Therefore, they need to be taken into account when a forecasting system is evaluated with regard to its practical usefulness.

5. Summary and conclusions

Good short-range DNI forecasts are highly demanded by solar energy producers, but are very difficult to achieve because of the large number of factors involved. Two of the most important factors are cloudiness and aerosol load. Current operational NWP models incorporate cloud schemes but continue to use climatological aerosol values.

To address this problem we propose a relatively simple and effective method based on libRadtran simulations for clear-sky fed with aerosol forecasts combined with a forecast clearness index calculated from NWP

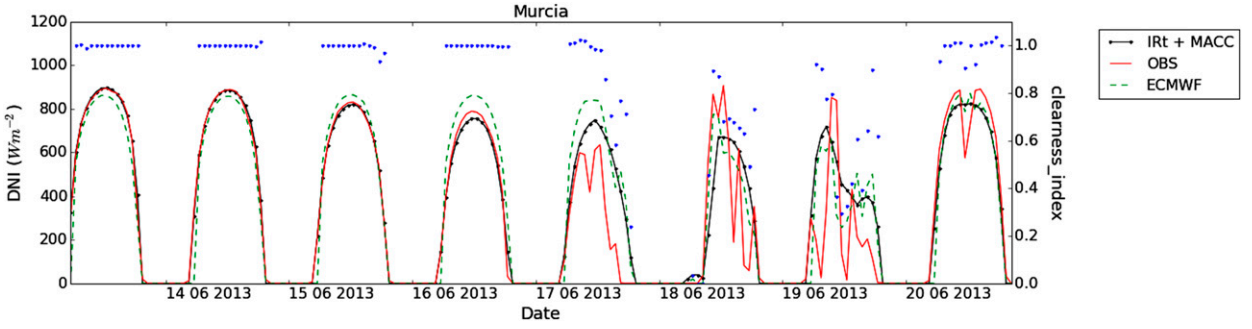

FIG. 6. DNI for 13–20 Jun 2013 in Murcia, comparing ECMWF 1-h (green dashed), libRadtran with MACC (black continuous with dots), and observations (red continuous). Blue dots indicate the clearness index.

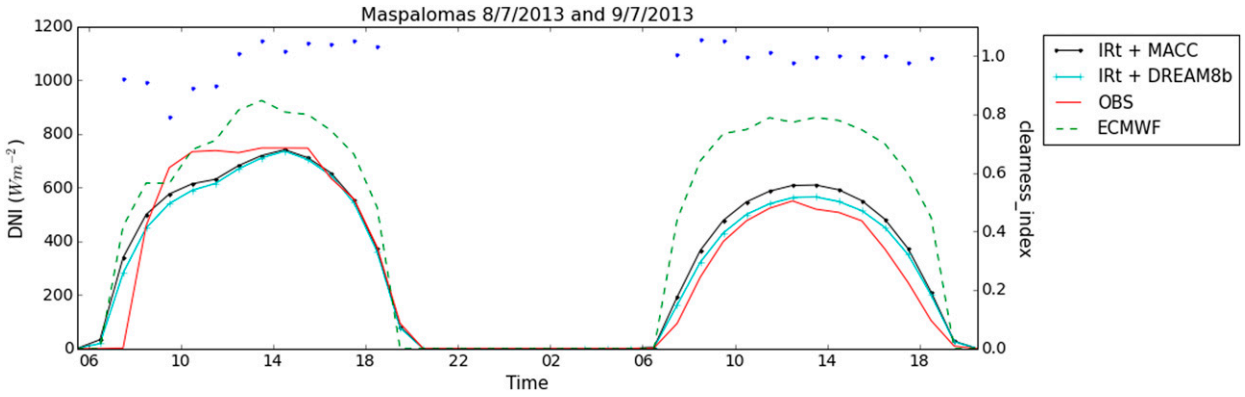

FIG. 7. DNI for 8–9 Jul 2013 in Maspalomas, comparing ECMWF (green dashed) and libRadtran with MACC (black with dots) and with BSC-DREAM8b (light blue with plus signs) against observations (red continuous). Blue dots indicate the clearness index.

direct radiation forecasts. This method makes it possible to obtain a stable and continuous DNI forecast. It avoids the use of different methods for different meteorological situations, which can lead to artificial and abrupt changes in the predicted curve. It can be adapted quite easily to different NWP and aerosol models and run for long periods with little computational cost. Therefore, it can be used as a diagnostic tool to check the effect of input variables on the accuracy of the predicted direct radiation or as an operational product. Furthermore, since it is a postprocessing method and not integrated within a model, it can be improved independently without affecting other parts of the NWP model.

As CSP plants usually only need DNI forecasts for specific sites, the point DNI predictions provided by our method are appropriate for them. Furthermore, information about cloudiness from nearby points is included by averaging the clearness index spatially.

The optimal spatial resolution for the clearness index has been studied in detail. High variability has been found depending on the orography of every site. The optimal grid varies in a range of 50–250 km. For inland sites, a positive correlation has been found between the RMSE of the forecast and the distance of the site to the nearest mountains.

The method has been validated against DNI observations at eight stations in Spain in areas with high solar resources, using the ECMWF as the input NWP model. Two types of aerosol forecasts have been tested: AOD550 from the global model MACC, which includes five major aerosol components, and the dust AOD550 from the regional model BSC-DREAM8b added to a background calculated from independent AERONET data. The ECMWF model has been used as reference with which to compare this combined model.

When this combined method was used, DNI forecasts improved by 5%–12% annually when compared with ECMWF forecasts. The study of monthly variations shows that the seasonal evolution of this improvement depends greatly on the location and also varies for different years. This shows that multiyear verification periods and sites with different climatologies are necessary to draw reliable conclusions. The rRMSE shows high correlations with the total cloud cover forecast on inland locations, which suggests the strong dependence of the combined method upon the cloud forecasts used.

Clear-sky situations and high aerosol load events have also been studied separately. In all cases, the results indicate the dominance of cloudiness in radiation attenuation. However, the DNI reduction attributable to aerosols is by no means negligible and has been found to be close to 50% under specific scenarios. Although dust models can be useful for radiation forecasting in areas where dust accounts for a high proportion of the total aerosol, in general aerosol descriptions with more prognostic components are needed to capture relevant events and achieve better predictions of DNI.

Acknowledgments. The authors acknowledge the libRadtran developers for their radiative transfer tools used in this work and ECMWF for their forecasts. We thank the MACC project, funded by the European Commission under the EU-Horizon 2020 Programme and coordinated by the ECMWF, for their AOD data, freely available on its website (http://www.gmes-atmosphere.eu/). Dust forecasts from the BSC-DREAM8b, operated by the Barcelona Supercomputing Center (http://www.bsc.es/projects/earthscience/BSC-DREAM/) have been used. AERONET provided observational data. We thank all the PIs and their staff for establishing and maintaining the sites used in this investigation. We also thank the Group of Atmospheric Optics, Valladolid University, for the provision of the CAELIS tool (http://www.caelis.uva.es) used in this publication, and the Forecast and Load

Scheduling Department from Red Eléctrica de España for their useful comments.

REFERENCES

Basart, S., C. Pérez, S. Nickovic, E. Cuevas, and J. Baldasano, 2012: Development and evaluation of the BSC-DREAM8b dust regional model over northern Africa, the Mediterranean and the Middle East. *Tellus*, **64B**, 18539, doi:10.3402/tellusb.v64i0.18539.

Beyer, H., J. Martinez, and M. A. Suri, 2009: Report on benchmarking of radiation products. Management and Exploitation of Solar Resource Knowledge (MESOR) Tech. Rep. 038665, European Commission 6th Framework Programme, 160 pp. [Available online at http://www.mesor.org/docs/MESoR_Benchmarking_of_radiation_products.pdf.]

Blanc, P., and L. Wald, 2016: On the effective solar zenith and azimuth angles to use with measurements of hourly irradiation. *Adv. Sci. Res.*, **13**, 1–6, doi:10.5194/asr-13-1-2016.

Breitkreuz, H., M. Schroedter-Homscheidt, T. Holzer-Popp, and S. Dech, 2009: Short-range direct and diffuse irradiance forecasts for solar energy applications based on aerosol chemical transport and numerical weather modeling. *J. Appl. Meteor. Climatol.*, **48**, 1766–1779, doi:10.1175/2009JAMC2090.1.

ECMWF, 2016: Part IV: Physical processes. IFS Doc. Cy43r1, 223 pp. [Available online at http://www.ecmwf.int/sites/default/files/elibrary/2016/17117-part-iv-physical-processes.pdf.]

Girodo, M., 2006: Solarstrahlungsvorhersage auf der Basis Numerischerwettermodelle (Solar irradiance forecasts based on numerical weather prediction models). Ph.D. thesis, University of Oldenburg, Oldenburg, Germany, 159 pp.

Gleeson, E., V. Toll, K. P. Nielsen, L. Rontu, and J. Mašek, 2016: Effects of aerosols on clear-sky solar radiation in the ALADIN-HIRLAM NWP system. *Atmos. Chem. Phys.*, **16**, 5933–5948, doi:10.5194/acp-16-5933-2016.

Jimenez, P. A., and Coauthors, 2016: WRF-Solar: Description and clear-sky assessment of an augmented NWP model for solar power prediction. *Bull. Amer. Meteor. Soc.*, **97**, 1249–1264, doi:10.1175/BAMS-D-14-00279.1.

Kraas, B., M. Schroedter-Homscheidt, and R. Madlener, 2013: Economic merits of a state-of-the-art concentrating solar power forecasting system for participation in the Spanish electricity market. *Sol. Energy*, **93**, 244–255, doi:10.1016/j.solener.2013.04.012.

Lara-Fanego, V., J. Ruiz-Arias, D. Pozo-Vázquez, F. Santos-Alamillos, and J. Tovar-Pescador, 2012: Evaluation of the WRF model solar irradiance forecasts in Andalusia (southern Spain). *Sol. Energy*, **86**, 2200–2217, doi:10.1016/j.solener.2011.02.014.

Manners, J., J.-C. Thelen, J. Petch, P. Hill, and J. Edwards, 2009: Two fast radiative transfer methods to improve the temporal sampling of clouds in numerical weather prediction and climate models. *Quart. J. Roy. Meteor. Soc.*, **135**, 457–468, doi:10.1002/qj.385.

Martin-Pomares, L., J. Polo, D. Perez-Astudillo, and D. A. Bachour, 2015: Validation of GHI and DNI predictions from GFS and MACC model in the Middle East. *Proc. ISES Solar World Congress*, Daegu, South Korea, International Solar Energy Society, 236–247.

Mayer, B., and A. Kylling, 2005: Technical note: The libRadtran software package for radiative transfer calculations—Description and examples of use. *Atmos. Chem. Phys.*, **5**, 1855–1877, doi:10.5194/acp-5-1855-2005.

Morcrette, J.-J., and Coauthors, 2009: Aerosol analysis and forecast in the European Centre for Medium-Range Weather Forecasts Integrated Forecast System: Forward modeling. *J. Geophys. Res.*, **114**, D06206, doi:10.1029/2008JD011235.

——, A. Benedetti, L. Jones, J. W. Kaiser, M. Razinger, and M. Suttie, 2011: Prognostic aerosols in the ECMWF IFS: MACC vs. GEMS aerosols. ECMWF Tech. Memo. 659, 32 pp. [Available online at http://www.ecmwf.int/sites/default/files/elibrary/2011/11277-prognostic-aerosols-ecmwf-ifs-macc-vs-gems-aerosols.pdf.]

Nabat, P., and Coauthors, 2015: Dust aerosol radiative effects during summer 2012 simulated with a coupled regional aerosol–atmosphere–ocean model over the Mediterranean. *Atmos. Chem. Phys.*, **15**, 3303–3326, doi:10.5194/acp-15-3303-2015.

Perez, R., S. Kivalov, J. Schlemmer, K. Hemker Jr., D. Renn, and T. E. Hoff, 2010: Validation of short and medium term operational solar radiation forecasts in the US. *Sol. Energy*, **84**, 2161–2172, doi:10.1016/j.solener.2010.08.014.

——, and Coauthors, 2013: Comparison of numerical weather prediction solar irradiance forecasts in the US, Canada and Europe. *Sol. Energy*, **94**, 305–326, doi:10.1016/j.solener.2013.05.005.

REE, 2015: The Spanish electricity system 2014. Red Eléctrica de España Tech. Rep., 150 pp. [Available online at http://www.ree.es/sites/default/files/downloadable/the_spanish_electricity_system_2014_0.pdf.]

Ruiz-Arias, J. A., J. Dudhia, and C. A. Gueymard, 2014: A simple parameterization of the short-wave aerosol optical properties for surface direct and diffuse irradiances assessment in a numerical weather model. *Geosci. Model Dev.*, **7**, 1159–1174, doi:10.5194/gmd-7-1159-2014.

Schroedter-Homscheidt, M., A. Oumbe, A. Benedetti, and J.-J. Morcrette, 2013: Aerosols for concentrating solar electricity production forecasts: Requirement quantification and ECMWF/MACC aerosol forecast assessment. *Bull. Amer. Meteor. Soc.*, **94**, 903–914, doi:10.1175/BAMS-D-11-00259.1.

——, A. Benedetti, and N. Killius, 2017: Verification of ECMWF and ECMWF/MACC's global and direct irradiance forecasts with respect to solar electricity production forecasts. *Meteor. Z.*, **26**, 1–19, doi:10.1127/metz/2016/0676.

Stamnes, K., S. C. Tsay, W. Wiscombe, and I. Laszlo, 2000: DISORT, a general-purpose Fortran program for discrete-ordinate-method radiative transfer in scattering and emitting layered media: Documentation of methodology. DISORT Rep. v1.1, 107 pp.

Tanré, D., and Coauthors, 2003: Measurement and modeling of the Saharan dust radiative impact: Overview of the Saharan Dust Experiment (SHADE). *J. Geophys. Res.*, **108**, 8574, doi:10.1029/2002JD003273.

Tegen, I., P. Hollrig, M. Chin, I. Fung, D. Jacob, and J. Penner, 1997: Contribution of different aerosol species to the global aerosol extinction optical thickness: Estimates from model results. *J. Geophys. Res.*, **102**, 23 895–23 915, doi:10.1029/97JD01864.

Troccoli, A., and J.-J. Morcrette, 2014: Skill of direct solar radiation predicted by the ECMWF global atmospheric model over Australia. *J. Appl. Meteor. Climatol.*, **53**, 2571–2588, doi:10.1175/JAMC-D-14-0074.1.

Wittmann, M., H. Breitkreuz, M. Schroedter-Homscheidt, and M. Eck, 2008: Case studies on the use of solar irradiance forecast for optimized operation strategies of solar thermal power plants. *IEEE J. Sel. Top. Appl. Earth Obs. Remote Sens.*, **1**, 18–27, doi:10.1109/JSTARS.2008.2001152.